ULTRASHORT DOMAIN PERIODICALLY POLED LITHIUM NIOBATE

Period April 15, 1998 to October 15, 1998

Final Report

sponsored by

The US Air Force Research Lab and

The European Office of Aerospace R&D

Contract N F61775-98-WE060

(SPC-98-4046)

Vladimir Ya. Shur

Report Date : 10/10/98

INSTITUTE OF PHYSICS & APPLIED MATHEMATICS

URAL STATE UNIVERSITY

EKATERINBURG, RUSSIA

REPORT DOCUMENTATION PAGE

Form Approved OMB No. 0704-0188

1. AGENCY USE ONLY (Leave blank)	2. REPORT DATE	3. REPORT TYPE AND DATES COVERED
	10 October 1998	Final Report

4. TITLE AND SUBTITLE

Ultrashort domain periodically poled lithium niobate

5. FUNDING NUMBERS

F61775-98-WE060

6. AUTHOR(S)

Prof. Vladimir Ya. Shur

7. PERFORMING ORGANIZATION NAME(S) AND ADDRESS(ES)

Institute of Physics & Applied Math; Ural State University
Lenin Ave. 51,
Ekaterinburg 620083
Russia

8. PERFORMING ORGANIZATION REPORT NUMBER

N/A

9. SPONSORING/MONITORING AGENCY NAME(S) AND ADDRESS(ES)

EOARD
PSC 802 BOX 14
FPO 09499-0200

10. SPONSORING/MONITORING AGENCY REPORT NUMBER

SPC 98-4046

11. SUPPLEMENTARY NOTES

12a. DISTRIBUTION/AVAILABILITY STATEMENT

Approved for public release; distribution is unlimited.

12b. DISTRIBUTION CODE

A

13. ABSTRACT (Maximum 200 words)

In nonlinear optics applications employing quasi-phasematching, short-pitch domain gratings are generally required for the efficient generation of visible and ultraviolet light. Here we introduce an enhanced electric-field poling technique which incorporates spontaneous backswitching and leads to uniform short-pitch bulk domain structures. The total volume of backswitched material, and hence the duty cycle of the back-switched domain grating, can be controlled. Backswitched domain periods down to 2.6 microns are demonstrated in 0.5 mm thick LiNbO3 substrates..

14. SUBJECT TERMS

EOARD, Non-linear Optical Materials , Non-linear Optics, Poling of ferroelectrics,

15. NUMBER OF PAGES

33

16. PRICE CODE

N/A

17. SECURITY CLASSIFICATION OF REPORT	18. SECURITY CLASSIFICATION OF THIS PAGE	19, SECURITY CLASSIFICATION OF ABSTRACT	20. LIMITATION OF ABSTRACT
UNCLASSIFIED	UNCLASSIFIED	UNCLASSIFIED	UL

OUTLINE

ABSTRACT

In nonlinear optics applications employing quasi-phasematching, short-pitch domain gratings are generally required for the efficient generation of visible and ultraviolet light. Here we introduce an enhanced electric-field poling technique which incorporates spontaneous backswitching and leads to uniform short-pitch bulk domain structures. The total volume of backswitched material, and hence the duty cycle of the backswitched domain grating, can be controlled. Backswitched domain periods down to 2.6 μm are demonstrated in 0.5-mm-thick $LiNbO_3$ substrates.

INTRODUCTION

Recently a new branch of ferroelectric technology and science named domain engineering has been developing rapidly. It is aimed at production of desired reproducible domain structures in commercially available ferroelectric materials. Ferroelectric domain engineering is important for quasi-phasematched (QPM) nonlinear optics which requires the short-period domain gratings [1]. Electric field poling at room temperature, first applied to bulk $LiNbO_3$ by Yamada et al. [2], has become conventional due to its repeatability and applicability over a wide range of nonlinear optical materials. To date the creation of the domain period of 3-4 μm in 200 - 300 μm thick substrates have been reported for electric field poled $LiNbO_3$ [3], $LiTaO_3$ [4,5] and KTP [6] which shows promise for blue and even UV light applications. Nevertheless, in thicker substrates, remain difficulties to prepare QPM materials for visible and UV wavelengths. The field induced development of the domain structure in $LiNbO_3$ is practically unstudied due to extremely high value of the threshold field (more than 21 kV/mm at room temperature). As all domain patterns in ferroelectrics obtained during switching in external field are of kinetic nature [7], the comprehensive study of domain evolution at different stages of poling process is required to improve the conventional technique.

We investigate formation and stabilization of the bulk domain patterns produced in $LiNbO_3$ by application of a high field to photolithographically-defined periodic electrodes. Visualization of the domain patterns by SEM and optical microscope, mathematical treatment of the poling current data and computer simulation of domain kinetics are used for analyzing of the stages of domain patterning. The domain evolution during spontaneous backswitching after removing/decreasing of the poling field is explored. We demonstrate that controlled backswitching can be used as a powerful tool for producing the high quality short-pitch domain patterns with periods up to 2.6 μm in 0.5-mm-thick $LiNbO_3$ substrates needed for quasi-phase matching devices.

EXPERIMENT

The periodic bulk domain structures are obtained in standard optical-grade single-domain 0.5-mm-thick $LiNbO_3$ wafers of congruent composition cut perpendicular to polar axis. The substrates are photolithographically patterned with periodic strip metal-electrode (NiCr) structure deposited on $\mathbf{z}^+$ surface only. The patterned surface is overcoated with a thin insulating layer (photoresist or spin-on-glass) to inhibit domain growth between the strip electrodes (Fig. 1).

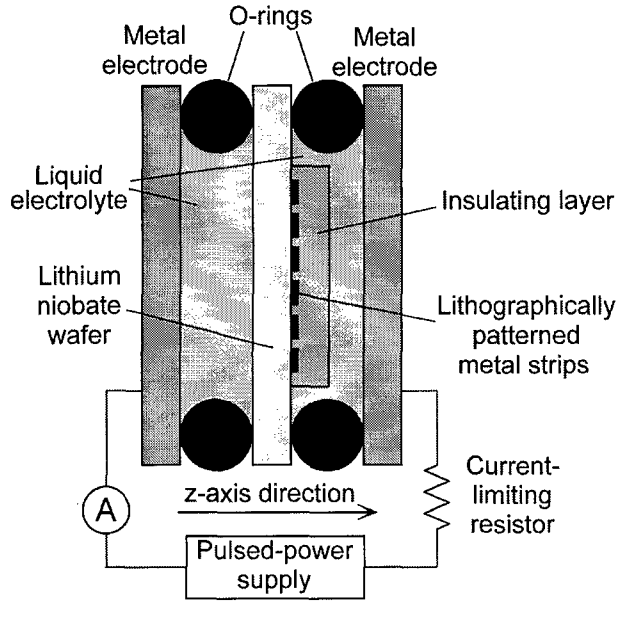

FIGURE 1 Scheme of the experimental setup for poling.

A high voltage pulse producing an electric field greater than the threshold ("coercive") field (21.5 kV/mm) is applied to the structure through the fixture containing a liquid electrolyte (LiCl) [8,9]. Both the voltage and current are monitored during the poling. The parameters of the domain structure are controlled by the pulse shape and current value. After complete or partial poling the polar surfaces and cross-sections are etched for 5 - 10 minutes by hydrofluoric acid (without heating). The surface relief associated with domain patterns is visualized by optical microscope and SEM. Studying the domain structure in the bulk by optical method the spatial resolution in **x** direction is enhanced by choosing appropriate tilted cross-sections. The comparison of domain patterns obtained for different duration of the poling pulse yield the information about the stages of domain evolution.

Always we use the single pulse poling ("switching") (Fig. 2). Pulse duration depends on the sample area due to the current limitation. The waveform for conventional poling is

presented on Fig. 2a. The duration of additional "stabilization" stage is chosen so as to prevent the spontaneous domain reversion to their original configuration after removing of the poling field ("backswitching process"). This method allows to fabricate the nonlinear device chips with high yield and reproducible characteristics in 0.5 mm thick by 50 mm long samples based on processing of 3 inch diameter $LiNbO_3$ wafers [10]. The obtained domain periods of 10 to 30 microns are suitable for infrared devices [8,10]. Recent optimization of this method makes it possible to achieve the periods up to 6.5 microns with duty cycles about 0.3 [11].

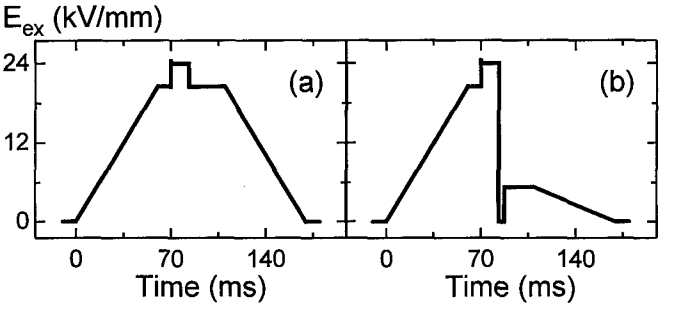

FIGURE 2 Poling voltage waveforms for (a) conventional poling and (b) backswitching one.

The shorter periods and increasing of the sample thickness are required for enlarging the areas of application. There are some principal obstacles on this way. The typical domain patterns on z^+ show the significant domain enlarging (shift of the domain walls) out of electroded area which is difficult to control. For high spatial frequency this shift can lead to the merge of domains on z^+. Moreover as a rule the domain wall shape is irregular. The patterns at z^- always differ as compare to z^+ and for a short period electrode structure the periodical domain patterns on z^- are not obtained.

3D analysis of the domain patterns

In order to improve the spatial resolution of optical method for observation the details of 3D lamellar-type structures we have studied the patterns etched at the tilted cross-sections of the poled samples.

1. The tilt from the conventional direction (perpendicular to electrodes) for about 80^o allows to obtain the 6 times blow up of the lamellar-type structure sizes in **x** direction which allows to resolve the shape peculiarities of the domain structure (Fig. 3). Such details of the domain shape were inaccessible during optical observation of the conventional (normal to electrodes) cross-sections.

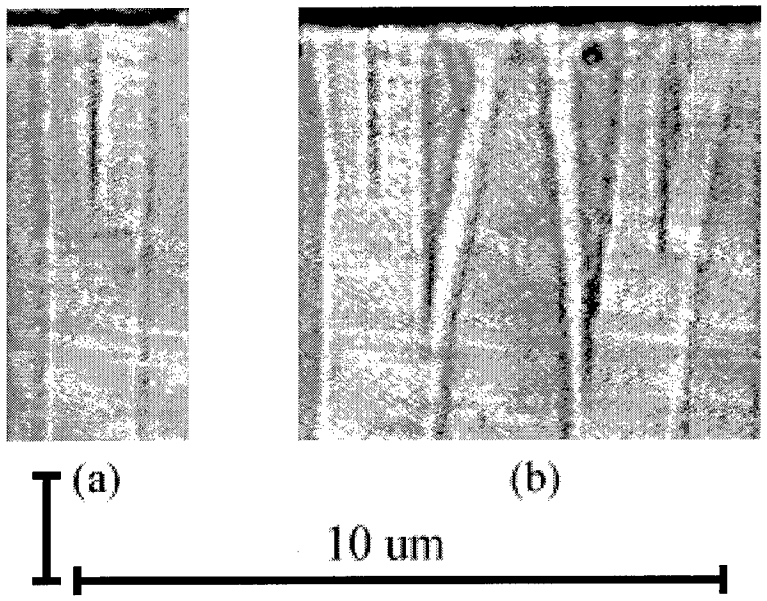

FIGURE 3 Domain changing by backswitching for 4 μm period (y surface, tilted cross-section): (a) -"erasing" and (b) - "splitting".

2. The additional tilt in the general direction (Fig. 4) allows to carry out the statistical analysis providing us with the knowledge of the domain structure evolution during tips propagation in polar direction.

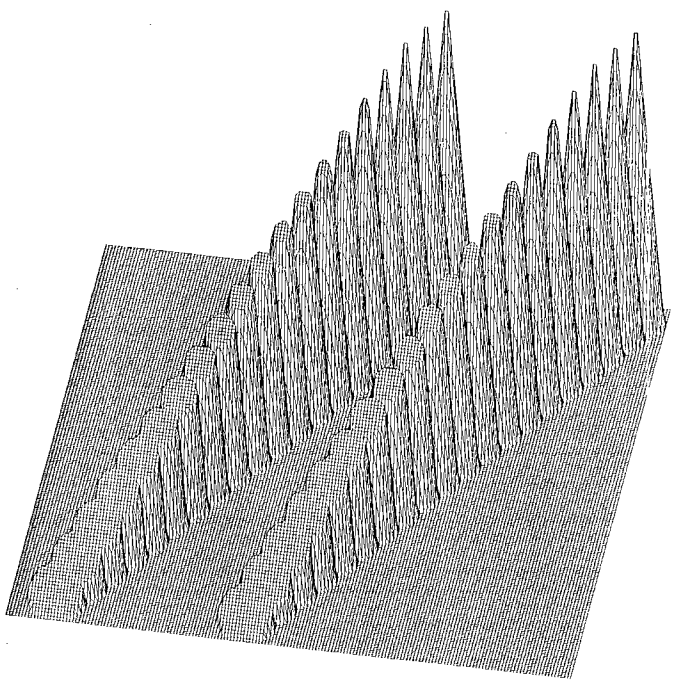

FIGURE 4 Computer simulation of 3D image demonstrated the tilted cross-section of the domain structure.

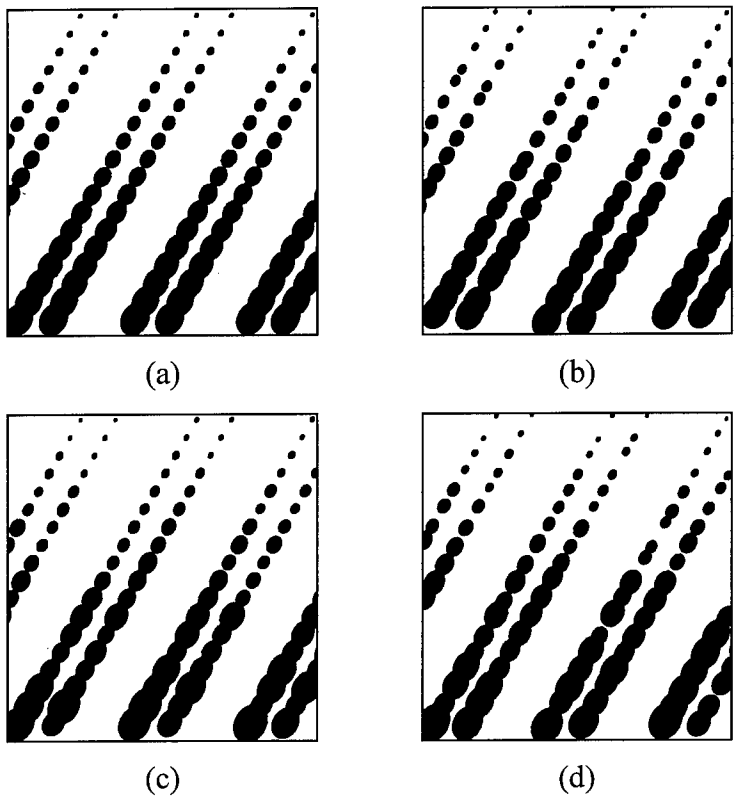

FIGURE 5 Computer simulation of the tilted cross-sections of the domain structure for the different model cases: (a) and (c) - correlated nucleation, (b) and (d) - random nucleation, (a) and (b) - β model; (c) and (d) - α model.

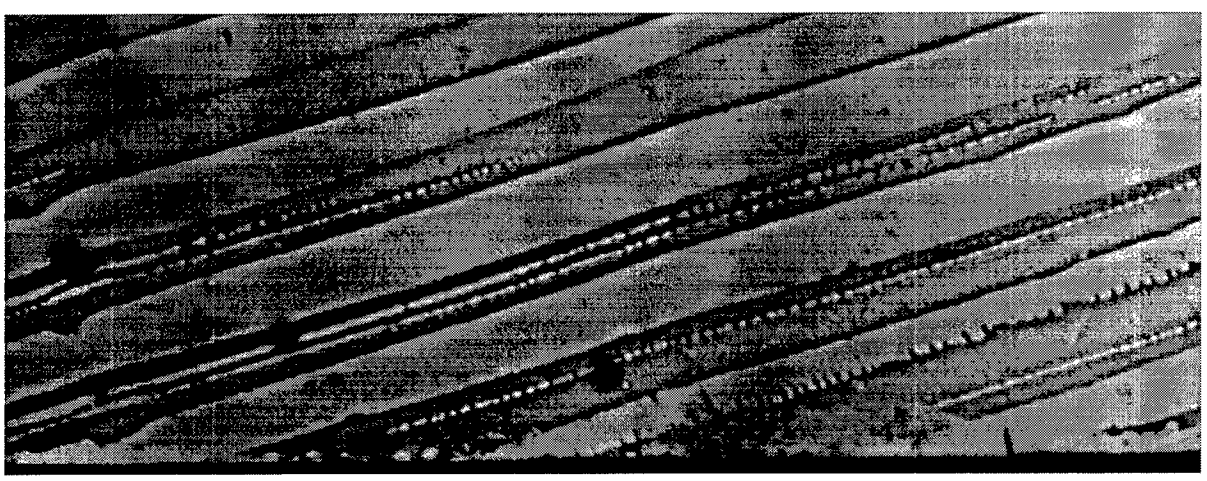

FIGURE 6 Experimental pattern of the domain structure visualized by etching on the tilted cross-section.

Experimental patterns obtained by tilted cross-sections were examined by computer image processing (Fig. 5) and compared with the computer simulation data (Fig. 6).

For the first time we have yielded such important parameters of the domain evolution during poling as: nuclei density and the sizes of the growing spike-like domains. The strong correlation in special distribution of nuclei is demonstrated on the Fig. 7, which presents the

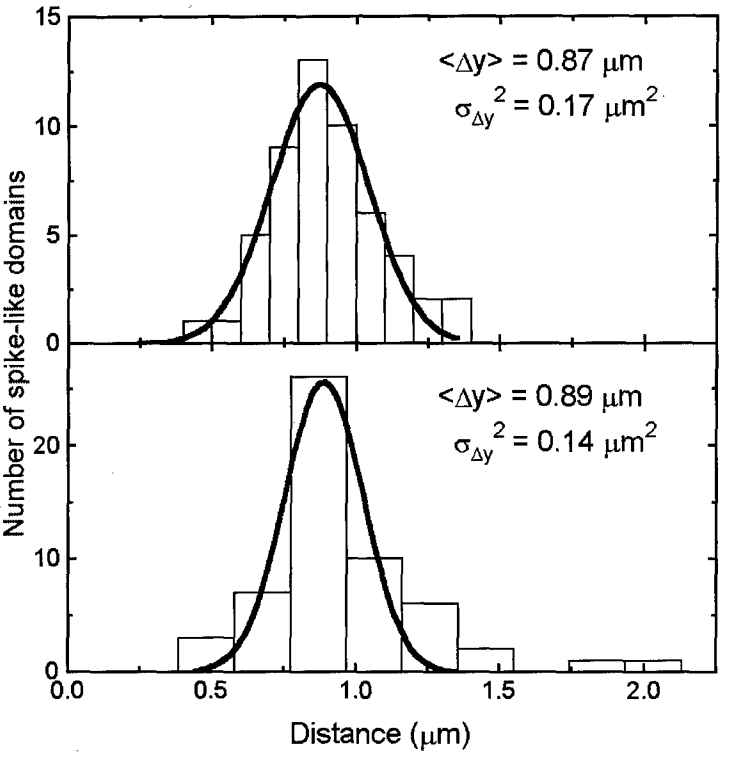

FIGURE 7 The histogram of the distances between the neighboring spike-like domains fitted by the Gaussian with average distances and dispersions.

histogram of the distances between the neighboring spike-like domains. The statistical results obtained by both these methods are summarized in the Tables 1 and 2.

TABLE 1.

1	Distance between spikes	0.91 ± 0.04 μm
2	Linear nuclei density	$(1.1 \pm 0.2)10^3$ mm^{-1}
3	Spike length	52 ± 6 μm
4	Spike angle	~1°

TABLE 2.

№	Sample	Average distance between spikes, μm	Dispersion, μm^2
1	R_503_7_3_2	0.94	0.03
2	R_b2_11_1	0.89	0.02
3	R_b2_11_2	0.88	0.03
4	R_b2_15_1	0.96	0.03
5	R_b4_03_2a	0.87	0.09

STAGES OF THE DOMAIN EVOLUTION DURING POLING

The analysis of the domain patterns after partial poling and backswitching makes it possible to distinguish several stages of domain evolution [12]. The brief scheme of the experimentally observed domain patterns at the stages is presented on Fig. 8. The poling process starts when polar component of the local field E_z exceeds the threshold value with the "nucleation" (arising of new domains) at $\mathbf{z}^+$ polar surface along the electrode edges [7] (Fig. 8a). The second stage represents forward and sideways growth and merging of the domains under the electrodes (Fig. 8b). At the end of the stage the laminar domains are formed (Fig. 8c). At the third stage the plane walls of laminar domains move out of electrodes (Fig. 8d).

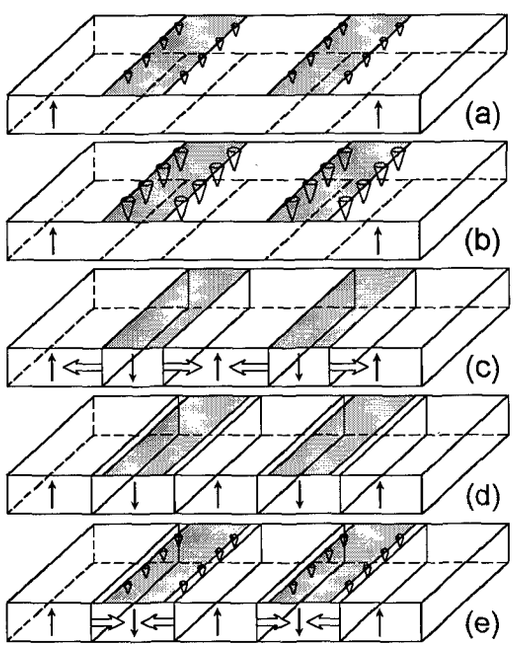

FIGURE 8 The main stages of domain evolution during switching in single domain plate with stripe electrodes. White arrows - directions of wall motion.

After termination of the switching process by rapid decreasing of the poling field two possibilities can be realized, depending on the duration of the switching pulse: either the stabilization of generated domain structure or the partial backswitching ("flip-back") of domains to initial state [10,13]. During backswitching poling the walls of switched laminar domains move in the opposite direction, additionally the domain chains arise and grow under the edges of electrodes (Fig. 8e).

MAIN APPROACH

Our approach to kinetics of domain patterning in the bulk ferroelectrics is based on the assumption of key role of screening effects [13]. It is clear, that switching from the single domain state is achieved through nucleation and growth of reversal domains [7]. Both nucleation and growth are governed by the polar component of local electric field E_z [7,13] at the nucleation sites and domain walls respectively. The spatial distribution of the local field E_z (r,t) is determined by the sum of **z** components of: 1) external field $E_{ex}(r)$ produced by the voltage applied to the electrodes, 2) the depolarization field $E_{dep}(r,t)$ produced by bound charges of instantaneous domain pattern, and 3) screening fields of two types: the external one $E_{escr}(r,t)$ due to the charge redistribution at the electrodes and the bulk one $E_{bscr}(r,t)$ which compensate the residual depolarization field by various bulk mechanisms [7,14,15].

$$E_z(r,t) = E_{ex}(r) - [E_{dep}(r,t) - E_{escr}(r,t) - E_{bscr}(r,t)] \quad (1)$$

The depolarization field slows the domain growth while the screening processes reduce its influence. It is important to keep in mind that after complete external screening the bulk residual depolarization field $E_{dr}(r)$ remains due to the surface dielectric gap existing in any ferroelectric [7,15].

$$E_{dr}(r) = E_{dep}(r) - E_{escr}(r) \neq 0 \quad (2)$$

For an infinite single-domain ferroelectric capacitor

$$E_{dr}(r) = 2LP_S(\varepsilon_L\varepsilon_o d)^{-1} \quad (3)$$

where L - thickness of dielectric gap, d - thickness of the sample,

P_S - spontaneous polarization, ε_L - dielectric permittivity of the gap.

This residual field can be screened by the charge redistribution in the bulk and aligning of polar defects [14,15]. These processes are relatively slow ($\tau \sim 10^{-1}$-10^5 s) [7] and usually obtained retardation of the bulk screening leads to various memory effects [13]. For example, after fast enough decreasing of the external field, the spontaneous backswitching process can partially or completely reconstruct the initial domain state. This process is determined by action of partially screened residual backswitched field.

$$E_{bs}(r,t) = -[E_{dr}(r) - E_{bscr}(r,t)] \quad (4)$$

It is shown by us that the manipulation by screening effects can be used to enhance the fidelity of fine-pitch domain structures [12].

MECHANISMS OF THE DOMAIN EVOLUTION

Nucleation of new domains at the surface

It is clear that nucleation density is the main parameter which is important for short-pitch domain gratings. Many attempts to increase it showed its weak dependence on the electrode material [9,16]. At the same time our experiments demonstrate that for the electrode gratings the surface density of spike-like domain nuclei is spatially nonuniform: far from the electrode edges it never exceeds 1000 mm^{-2} [16] and the nucleation dramatically increases along the electrode edges (Fig. 9a). Our analysis of the domain patterns during backswitching demonstrates that the typical linear density of arising spike-like domains is about 1100 mm^{-1}.

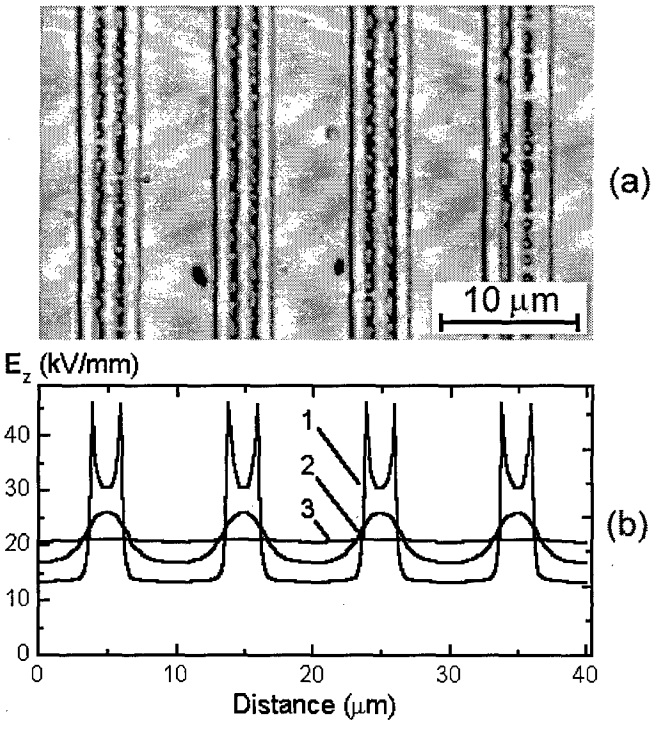

FIGURE 9 Nucleation near the edges of the electrodes (during backswitching) (a) and calculated spatial distribution of the field polar component E_z near $\mathbf{z}^+$ surface (b).

This behavior can be explained in framework of our approach by estimated singular spatial distribution of the polar component of switching field E_z at the surface near the edges of finite electrodes (Fig. 9b). It must be pointed out that spatially nonuniform $E_z(x)$ exists only in the vicinity of the surface and its amplitude rapidly decreases with the depth (Fig. 9b). Practically uniform field is obtained at the depth about the electrode period. Such estimations clarify the cause of observed spatially nonuniform nucleation in thin surface layer and show that subsequent growth of domains in the bulk goes on in uniform electric field.

The detail investigations of the beginning of spontaneous backswitching by visualization of the domain patterns at $\mathbf{z^+}$ using SEM allow to discover existence of the chains of nanodomains (Fig. 10). Typical diameter of the domains is about 50 - 100 nm with linear density up to 10^4 mm^{-1}. We propose that conventionally observed spike-like domains are formed as a result of growth of these nanodomains. The static individual needle-like microdomains less than one micrometer in diameter of unknown formation mechanism were observed in single domain $LiNbO_3$ earlier [17].

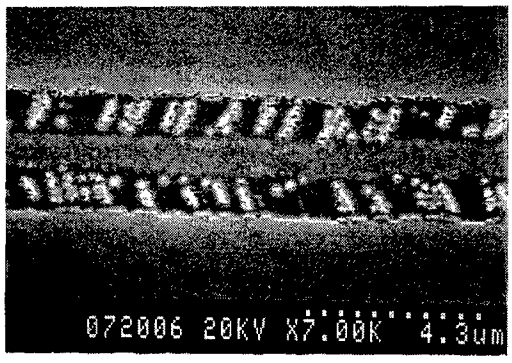

FIGURE 10 Nanodomain chains arising during backswitching (SEM visualization).

The analysis of experimental domain patterns at the first stage of poling/backswitching reveals the strong correlation in spatial distribution of the spike-like domains (Fig. 7). This effect can be explained while taking into account suppression of the local field in the vicinity of switched domain [7]. Such change of the spatial distribution of electric field suppresses the growth of the neighboring nuclei. This effect leads to correlated spatial distribution of the forming spike-like domains and to decreasing of their number as compare with the number of nuclei.

Forward growth and merging of spike-like domains under the electrodes

The enlargement of the nucleated spike-like domains is achieved through the forward (in polar direction) and sideways domain wall motion. The analysis of the static domain patterns observed on the tilted cross-sections shows that the ratio between the forward growth velocity $\mathbf{v_f}$ and the sideways one $\mathbf{v_s}$ is more than 100. This ratio determines the observed value of an angle at the top of the domain spikes being smaller than one degree.

For simultaneous growth of the spikes the value of $E_z(r,t)$ at the given tip depends on the distances from the neighboring domains. So local deviations of direction of moving spike

propagation are obtained due to variation of local field near the tip when its neighbor stops or is hampered by the defects. This effect can be partly responsible for usually observed difference between $\mathbf{z}^+$ and $\mathbf{z}^-$ domain patterns.

Analysis of the patterns observed on polar surfaces shows that the growing domains in $LiNbO_3$ are of hexagonal shape (Fig. 11a). For explanation of the growth of regular-shaped domains we take into account the similarity of two processes:domain enlargement and growth of regular crystals [18,19]. Domain growth (sideways motion of the domain walls) is then a layer-by-layer growth through propagation of individual steps along the walls (Fig. 11b). In $LiNbO_3$ existence of trigonal anisotropy in the plane normal to the polar direction leads to the preferable step propagation in three **y** directions [18]. Six plane domain walls are formed as a result of such growth (Fig. 11b). It must be pointed out that crystal anisotropy leads also to the formation of the domain chains strictly oriented in three **y** directions (Fig. 12). It must be stressed that the pattern was obtained under application of the uniform electric field.

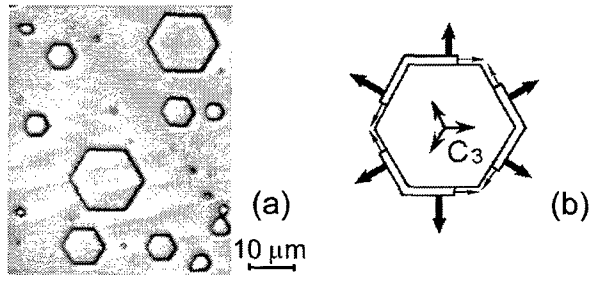

FIGURE 11 Hexagonal domains in $LiNbO_3$: experimental pattern (a), the scheme of layer-by-layer domain growth (b). Thin arrows – directions of step propagation; thick arrows – directions of wall motion.

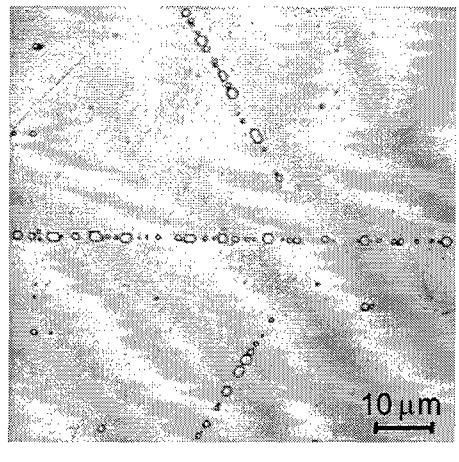

FIGURE 12 Oriented chains of domains arising in uniform electric field.

The orientation of strip electrodes is always chosen along one of the directions of preferential growth (step propagation). Due to such orientation the layer-by-layer growth prevail after merging of the domain chains, nucleated under the electrode edges at the first poling stage, leading to the forming of the couples of strip domains with plane walls at $\mathbf{z}^+$ surface. In thick substrates the coalescence of individual domains and formation of the strip ones at $\mathbf{z}^+$ terminates when the spike tips are still far from $\mathbf{z}^-$. Experiment shows that for the typical distance between nuclei about 0.9 μm the coalescence of isolated domains occurs when their tips grow in polar direction at the depth about 50 - 100 μm.

The pairs of domain walls formed along the edges of electrodes move towards each other until complete switching of the electroded area on $\mathbf{z}^+$. In 0.5-mm-thick substrates for electrode width less than 3 μm this coalescence terminates before the tips reach $\mathbf{z}^-$ surface.

The regular-shaped laminar domains are formed only after completion of the forward growth. Nevertheless the process of domain evolution does not terminated at this moment. Always the sufficient undesirable enlargement of the laminar domains out of electrodes is observed at the final stage.

Domain wall motion out of electrodes

The spread of the formed domain walls out of electrode for thick sample (when the electrode period $\Lambda << \mathbf{d}$) can be considered as a domain wall motion in uniform electric field. It is clear that the spatial inhomogenety of external field E_{ex} (which is so important for nucleation) exist only in the Λ-thick surface layer.

As considered above the wall velocity is determined by the polar component of local electric field E_z [20]. The ratio of compensation of depolarization field by external screening in the area between metal electrodes by charge redistribution at the liquid electrodes is smaller as compare with the compensation under the metal electrodes (Fig. 13). This effect and comparatively slow bulk screening in $LiNbO_3$ at room temperature leads to decrease of E_z during shifting due to increasing of uncompensated part of depolarization field. The domain wall stops when

$$E_z(\Delta x) - E_{th} \sim 0 \qquad (5)$$

where E_{th} - the threshold field for sideways motion of the plane domain wall,

Δx - wall shift out of electrodes.

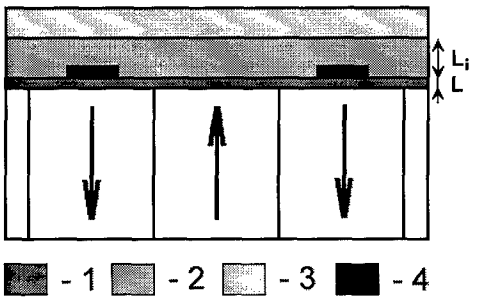

FIGURE 13 Scheme of the surface region of the substrate with electrodes. (1 - dielectric gap, 2 - insulating layer, 3 - liquid electrolyte, 4 - metal electrodes).

Assuming that conductivity of insulating layer and bulk screening can be ignored and that the thickness of insulating layer $L_i >> L$ the dependence of average bulk value of E_z on Δx can be estimated for used experimental setup (Fig. 13). The decrease of E_z during motion occurs due to the increasing of $E_{dr}(\Delta x)$ and the field produced by the "frozen" bulk screening charges (memory effect). If the charge spatial distribution is approximated by two strips of the width Δx with effective surface charge density σ, then the shift dependence of the field at the domain wall is [20].

$$E_z(\Delta x) = E_{ex} - E_{dep}(\Delta x) = U/d - \sigma(\varepsilon_i \varepsilon_o)^{-1} F(\Delta x/d) \qquad (6)$$

where U - applied voltage, ε_i - dielectric permittivity of insulating layer,

$$F(\Delta x/d) = 1/\pi[2 \operatorname{arctg}(\Delta x/d) + \Delta x/d \ln(1+d^2/\Delta x^2)],$$

$$\sigma = L P_S d^{-1} \varepsilon_b \varepsilon_L^{-1}(1 + k),$$

The parameter **k** takes into account the prehistory: for the first shift from completely screened state **k** = 1 and after long enough staying in the shifted state **k** = - 1.

The Equation (6) allows to determine the field dependence of the domain shift out of electrodes $\Delta x(E_{ex} - E_{th})$.

It is clear that conductivity of imperfect insulating layer destroys the proposed consideration leading to sufficient increase of the domain shift. As a result the observed wall shift can depend on the technology of deposition and composition of insulating layers.

The decreasing of the ratio of the external compensation of depolarization field in between the electrodes by optimization of the parameters of insulating layer and the shape of electrode edge is the way to prevent the undesirable domain broadening.

"Finger assisted" mechanism of domain wall motion.

We have found that for short period patterning the spreading amplitude often varies from electrode to electrode and abnormally large shifts occur in some regions (Fig. 14a). Such behavior can not be explained by the considered mechanism of plane domain wall motion.

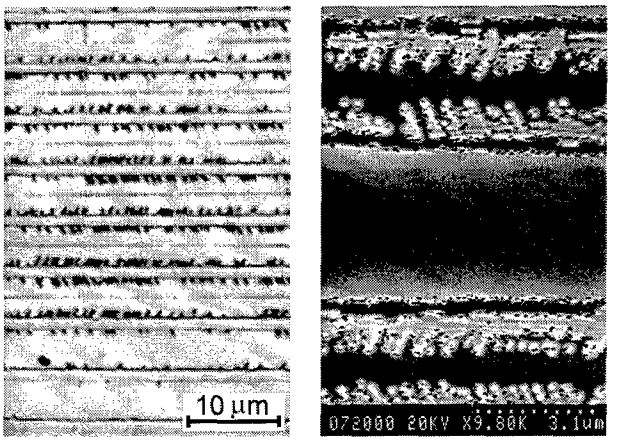

FIGURE 14 "Finger assisted" mechanism of domain spreading out of electrodes. Domain patterns observed by: optical microscope (a) and SEM (b).

For studying the early stages of domain evolution in this case we analyze the domain patterns after very short partial backswitching. This possibility is based on the experimentally confirmed fact that the domain nucleation during backswitching is similar to that for poling (switching). The observations of the domain patterns (relief of the etching surface) by optical microscope show that domain kinetics in this situation demonstrates arising, propagation and subsequent merging of the set of domain "fingers" oriented in one of **y** directions (Fig. 14a). The higher resolution observation by SEM shows that these optically observed domain fingers are really the chains of spike-like domains with diameter about 100 nm (Fig. 14b). The linear density of nuclei in chains is about 10^4 mm^{-1}. It is clear that for a short-pitch patterning this "finger assisted" mechanism of the wall motion leads to wall merging between electrodes and so to disruption of the periodicity of domain patterns.

The finger assisted mechanism of the wall motion can be considered in analogy with the correlated nucleation effect discovered by us in lead germanate [21,22]. This effect is due to the remote action of the moving domain wall. The calculation of $\Delta E_z(x)$ near the domain wall (Fig. 15) demonstrates a pronounced field maximum at a distance about thickness of the dielectric gap L [7]. In $LiNbO_3$ this peculiarity leads to formation of the oriented chains of spike-like nanodomains (fingers) in the surface layer. The subsequent growth and merging of

the fingers leads to abnormal motion of the domain walls and as a result to observed variations of local domain width (domain duty cycle) and wall shape.

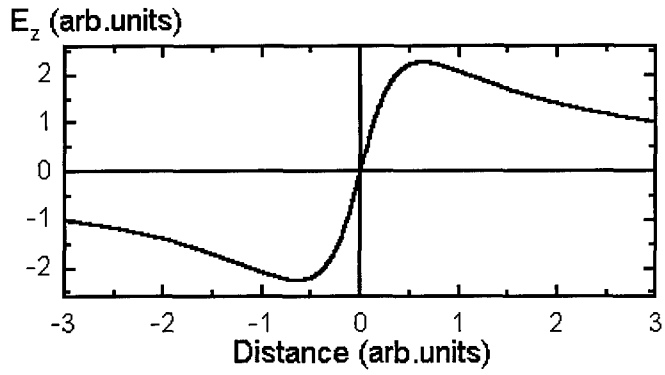

FIGURE 15 Spatial distribution of the polar component of the local field E_z (x) at the surface in the vicinity of the plane domain wall.

Evolution of the domain structure during backswitching process

In contrast to the conventional approach we demonstrate the opportunity to use the spontaneous backswitching for domain patterning [12]. This original approach to the problem is based on ideas experimentally confirmed in our works [7,13].

For domain patterning by backswitching poling we qualitatively modify the voltage waveform (Fig. 2b). As a result of application of the first (high-applied-field) part of the waveform the width of formed laminar domains sufficiently exceeds the width of electrodes. The backswitching process starts during the low-applied-field part through the domain wall motion of residual (nonswitched) domains. Moreover the nucleation and growth of spike-like domains under the edges of electrodes occurs so as during switching (Fig. 8a). The domain patterns produced by backswitching stage are "frozen in" during the stabilization part of the waveform but with the lower field value than during conventional poling (Fig. 2b). This method allows to freeze in the patterns corresponding to the different stages of backswitching process by the variation of the low-field part duration. The controlled shift of the plane domain walls of residual domains allows to generate short-pitch domain patterns with higher fidelity in thick substrates.

The pronounce role of correlated nucleation was observed during backswitching. The backswitching process starts by the quasi-periodical nucleation of backswitched domains along and just under the edges of electrodes on z^+ surface (Fig. 16a). The strong correlation in their spatial distribution is observed with average period about 0.9 μm (Fig. 7). After coalescence of isolated needle-like domains on z^+ surface the straight domain lines formed

along the electrode edges. At the next step of backswitching one more correlated nucleation took place. As a result two additional lines of isolated domains (chains) aligned along the electrode edges at the distance about 1 μm from the first straight domain lines are observed (Fig. 16b). Important that these domain chains appear outside of electroded area. Their merging leads to the formation of the additional straight domain lines (Fig. 16c). This effect opens the new possibility for the multiplication of the domain spatial frequency as compare with the electrode's frequency.

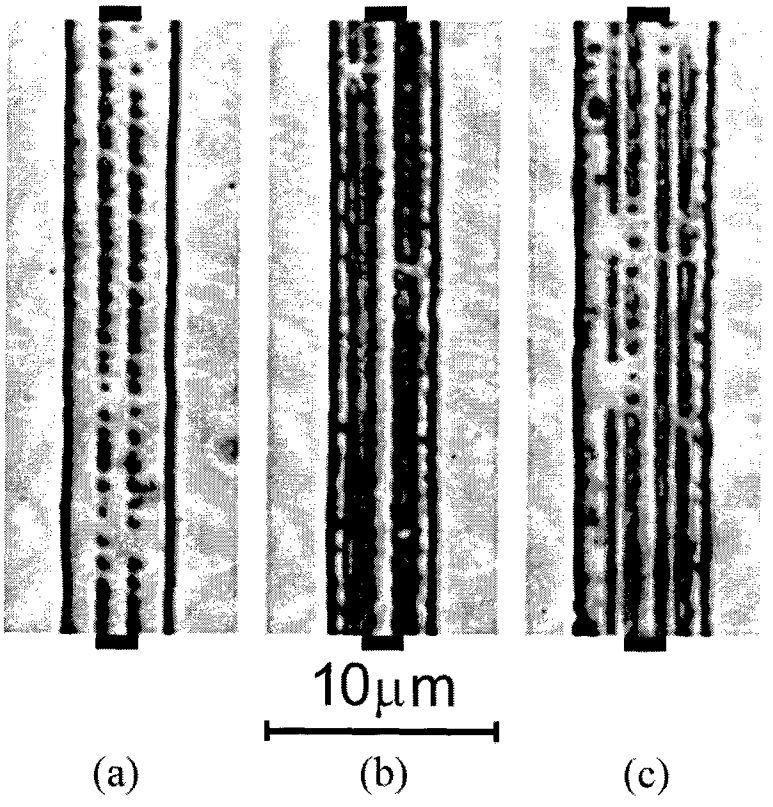

FIGURE 16 Correlated nucleation during backswitching. Domain patterns at the different stages of the domain evolution. Black rectangles show the positions of the electrodes.

The effect of the reproducible chains formation is determined by the specific spatial distribution of the local field in the vicinity of the formed straight line domains [11]. The calculation of the depolarization (backswitching) field distribution near the plane domain wall (Fig. 15) in this case also demonstrates the pronounced maximum but at the distance of about the thickness of the insulating layer [7].

Stabilization of the domain structure after poling

Any generated domain structure has to be stabilized using long enough exposure in constant electric field a bit lower than the threshold value (Fig. 2). Measurements of the dependence of the fraction of backswitched charge on the stabilization time demonstrate the exponential decrease with time constants from 10 to 30 ms (Fig. 17). Under the assumption that the depolarization field is the driving force of backswitching the stabilization kinetics must be determined by bulk screening time constant [13,14]. It was demonstrated experimentally that the stabilization step duration more than 50 ms is practically enough for complete blocking the backswitching process after removing of poling field [10].

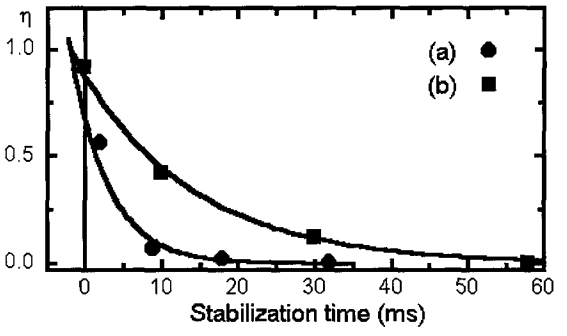

FIGURE 17 Dependence of the fraction of the backswitching charge on the stabilization time for different stabilization fields: (a) 24 kV/mm and (b) 20.6 kV/mm.

Frequency multiplication

The carried out complex investigations of the domain kinetics in $LiNbO_3$ make it possible to propose and use the qualitatively new method of domain patterning with multiplication of the domain pattern frequency as compare to the electrode one. This method is based on the above discussed effect of correlated nucleation during backswitching. We can obtain different variants of multiplication by varying the width of the electrodes and poled domains, and the duration of backswitching stage (Fig. 18).

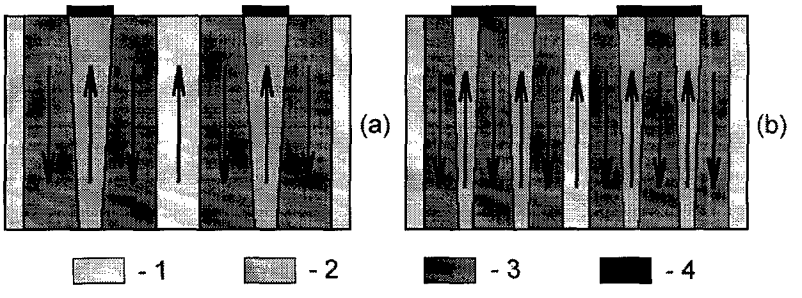

FIGURE 18 Scheme of the multiplication of domain pattern spatial frequency during backswitching: (a) "frequency doubling" and (b) "frequency tripling".

"Frequency doubling" can be obtained as a result of appearance of additional backswitched straight domain lines under the whole electrode on $\mathbf{z}^+$ (Fig. 19a). In this case the depth of backswitched domains depends on the pulse parameters and width of electrodes and typically is about 50 - 100 μm (Fig. 19b).

For wider electrodes we demonstrate the "frequency tripling" limiting the duration of backswitching stage (Fig. 19c). Under these conditions the additional domain "strips" with depth about 20 - 50 μm arise just under the edges of the electrodes (Fig. 19d).

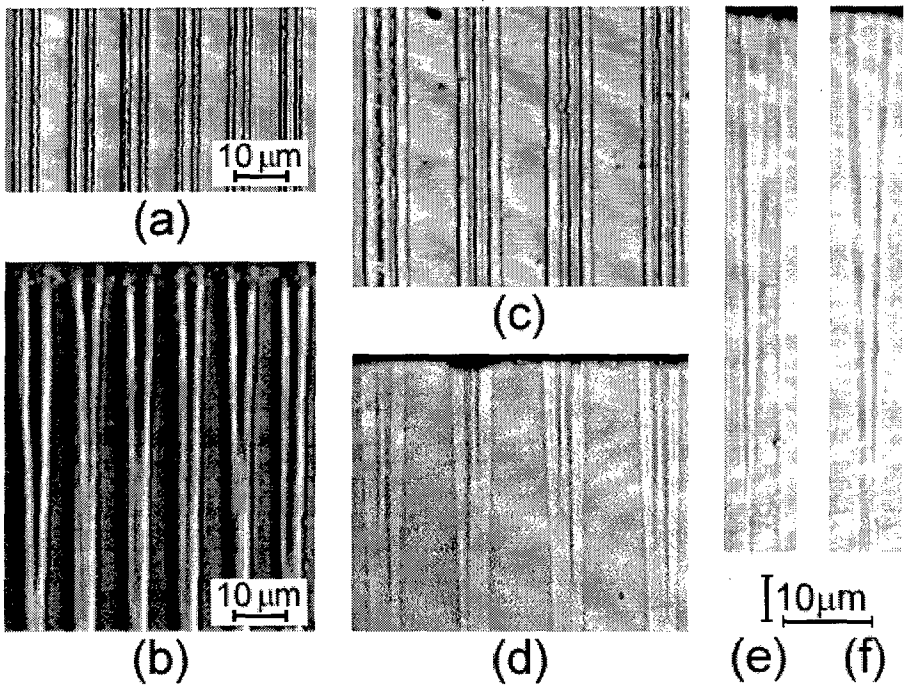

FIGURE 19 Results of backswitched poling. "Frequency doubling": $\mathbf{z}^+$ view (a) and **y** cross-section (b). "Frequency tripling": $\mathbf{z}^+$ view (c) and **y** cross-section (d). "Erasing" (e) and "splitting" (f) - tilted cross-sections.

For small electrode duty cycle and wide poled domains we obtain even the "frequency pentaplication" (Fig. 20 and 21). In this case the additional couple of the backswitched straight domain lines appear out of electroded area at the distance which is defined by the thickness of the insulating layer.

Detailed analysis of the cross-sections of backswitched domains reveals two distinct variants of their evolution during frequency multiplication: "erasing" and "splitting". The erasing process consists in formation of backswitched domains in earlier switched area without any variation of the external shape of poled domain (Fig. 19e). In contrast, during splitting the growing backswitched domains cut the initial poled one conserving its volume (Fig. 19f).

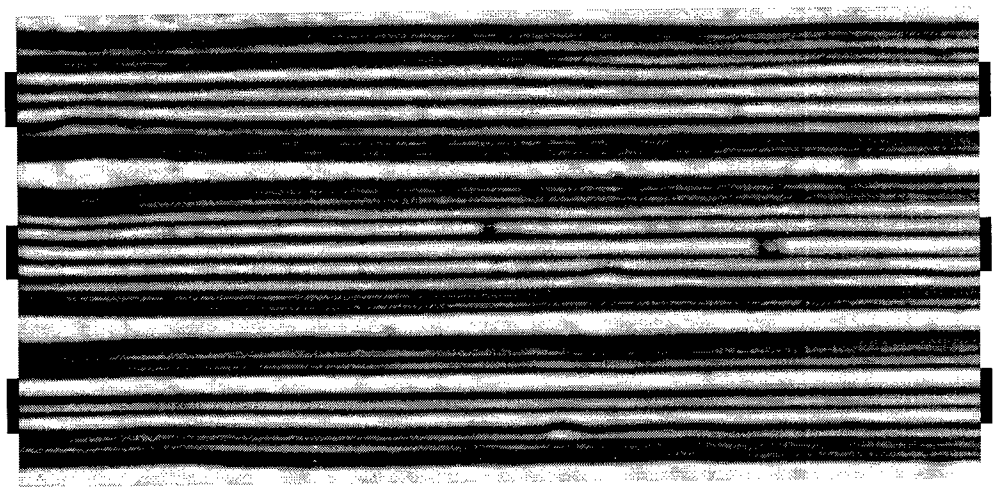

FIGURE 20 Results of backswitched poling. "Frequency pentaplication": $\mathbf{z}^+$ view, electrode period 7 μm. Domain pattern visualized by optical microscope. Black rectangles show the position of the electrodes.

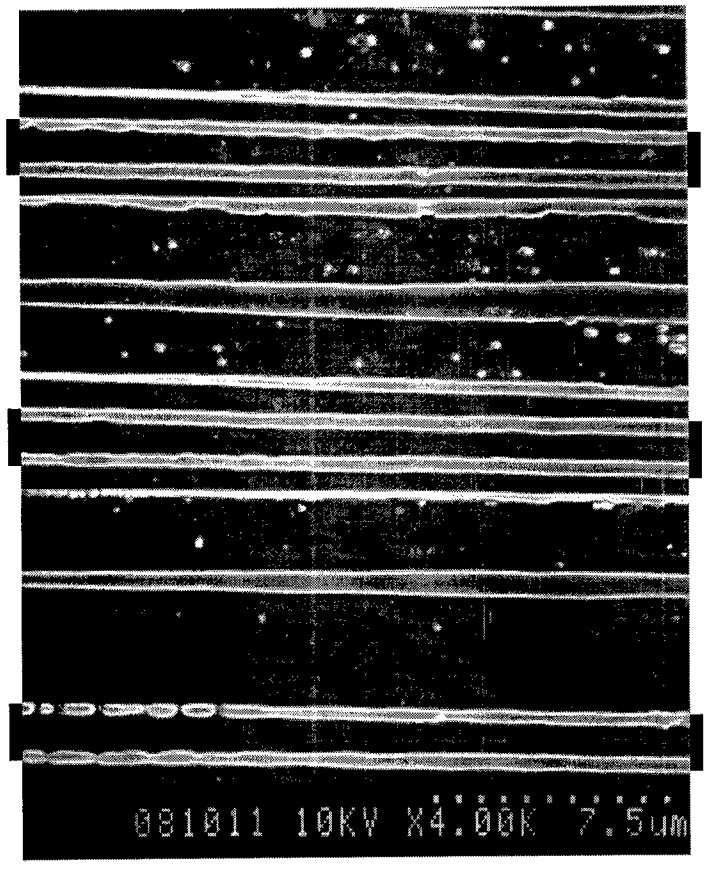

FIGURE 21 Results of backswitched poling. "Frequency pentaplication": $\mathbf{z}^+$ view, electrode period 7 μm. Domain pattern visualized by SEM. Black rectangles show the position of the electrodes.

ANALYSIS OF THE SWITCHING CURRENTS

In addition to the obtained local investigations of domain kinetics by visualization of the sequence of the domain patterns we use the *in situ* recording of the switching currents [23-25]. This method being rather simple and popular usually yield the restricted information. Moreover it was never used for extracting the information about the details of domain evolution. Our approach to analysis of the switching current data allows us to obtain the field dependence of the domain growth velocity during the comparatively fast switching in $LiNbO_3$ and to distinguish the main stages of domain evolution during domain patterning [23-25].

Switching in linear increasing field

For measurement of the switching currents in increasing field we use the conventional setup but without metal electrodes on the surface. In this case the switching area (about 3-10 mm^2) is controlled by the diameter of O-rings (Fig. 1). We choose the small switching area and low field increasing rate ($dE/dt = 0.2 \div 0.3$ $kV(mm \cdot ms)^{-1}$) to obtain switching data without current limits.

The analysis of domain patterns for partial switching shows that all domains arise only at the electrode edges and grow having hexagonal shape (Fig. 22a). It means that in this case the switching process starts from 2D domain growth and undergoes *the geometrical catastrophe* with the decrease of the growth dimensionality [24] after complete switching along the electrode edge. So during fitting we divide the whole switching data into two parts differ by geometry of domain growth.

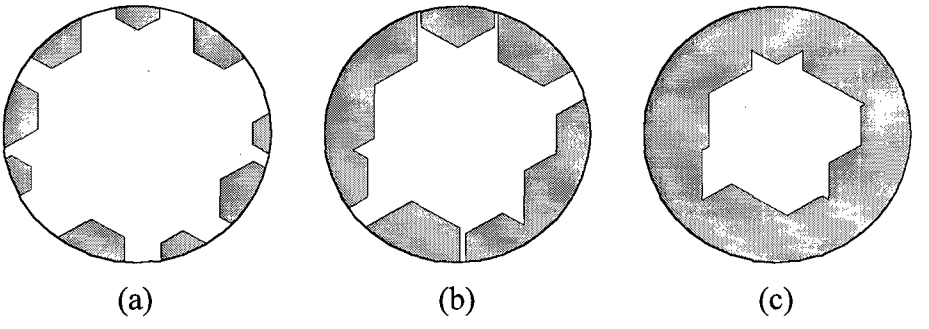

FIGURE 22 The stages of the domain evolution during poling under the circular electrode for nucleation only at the boundary of switching area and growth of hexagonal domains.

The time dependence of the switching current for 2D growth during switching in the linear increasing field and nucleation only at the boundary of the switching area can be fitted by the following formula [24,25]

$$j[E_{ex}(t)] = j_{max}\{1-\exp[-(t/t_o)^6]\} \quad (7)$$

where t_o - the time constant of the switching process.

After the geometrical catastrophe (complete merging of all isolated domains along the boundary) (Fig. 22b) the domain evolution is determined by the motion of the one domain wall (Fig. 22c). We can use the linear approximation of field dependence of the wall sideways motion velocity due to comparatively narrow range of poling fields

$$v(E_{ex}) = \mu\,(E_{ex} - E_{st}) \quad (8)$$

where μ - mobility of the domain wall, E_{st} - start field.

Then the following expression is obtained

$$j[E_{ex}(t)] = A\,(t - \Delta t) + B\,(t - \Delta t)^3 \quad (9)$$

where $\Delta t = E_{st}\,(dE_{ex}/dt)^{-1}$, $A/B = -R/(\mu\, dE_{ex}/dt)$, R - radius of switching area.

Fitting of experimental data by Equations (7) and (9) (Fig. 23) allows to extract the mobility of domain wall $\mu = 0.012 \pm 0.002$ cm^2/Vs and the start field $E_{st} = 23.4$ kV/mm.

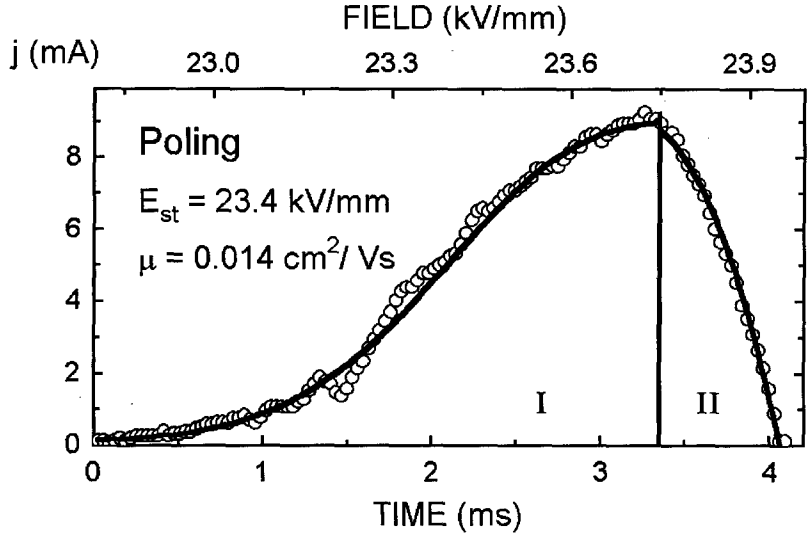

FIGURE 23 The switching current for poling under the circular electrode. The experimental points were fitted by Equations (7) and (9).

The observed deviations from the theoretical dependencies (especially at the first stage) can be attributed to the current jumps due to merging of the hexagonal domains (Fig. 22b) and abrupt change of the slope of current on time dependence at the moments of qualitative modification of domain wall shape (Fig. 22c).

It is important to compare the poling and repoling processes. It yield additional information about kinetics of bulk screening which determines the backswitching effect. The switching current recorded during repoling can be fitted by the same Equations (7) and (9) (Fig. 24). We have obtained the difference between the start fields values E_{st} which shows that the bulk screening in the interval between poling and repoling pulses (about 100 s) is still incomplete.

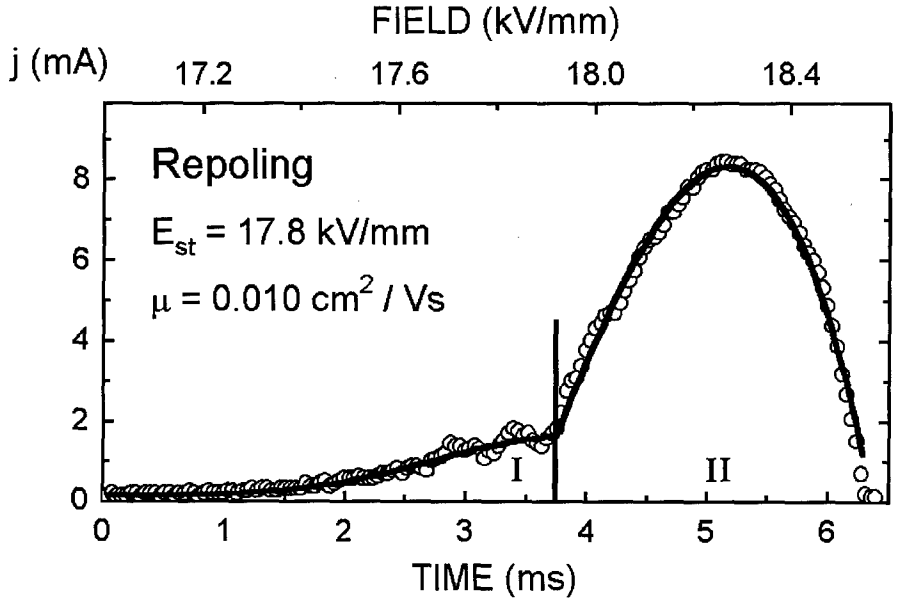

FIGURE 24 The switching current for repoling under the circular electrode. The experimental points were fitted by Equations (7) and (9).

Field dependence of the wall motion velocity

For clarifying the field dependence of the domain sideways motion velocity we use another method of mathematical treatment of switching current data. We analyze the time dependence of the switched area by integrating the current. Approximating the switched area by circle with radius R(t) it is easy to extract time dependence of wall motion velocity $v(t) \sim dR(t)/dt$. The obtained field dependence is typical for the nucleation assisted growth (Fig. 25)

$$v(E) = v_\infty \exp[-E_{ac} (E - E_b)^{-1}] \qquad (10)$$

where v_∞ - the extreme value of the velocity, E_{ac} - activation field, E_b - bias field.

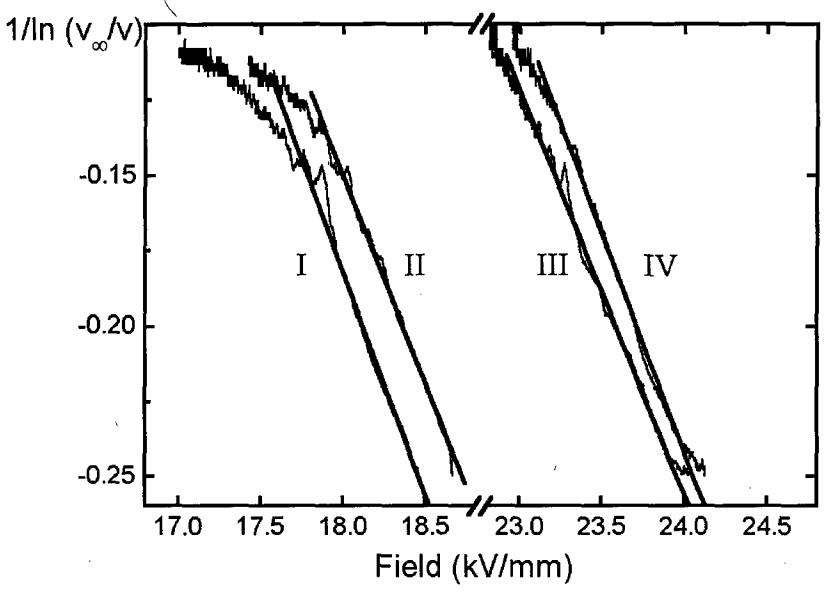

FIGURE 25 Voltage dependence of the domain wall sideways motion velocity extracted from the switching current data for poling under the circular electrode. The experimental points were fitted by Equation (10).

The main parameters extracted from the experimental data for different time intervals between poling and repoling (1 and 5 minutes) are presented in Table 3.

TABLE 3.

	E_b (kV/cm)	E_∞ (kV/cm)	E_b/E_∞	Process
I	16.52	7.40	2.23	repoling, 1 min
II	17.00	7.28	2.34	repoling, 5 min
III	22.20	7.84	2.83	poling, 1 min
IV	22.16	7.16	3.10	poling, 5 min

Switching current during domain patterning

Analysis of the switching current recorded during conventional poling using periodical strip electrodes (Fig. 26) requires the separation of the whole switching data into four inputs corresponding to switching currents accompanied polarization reversal in different parts of the sample (Fig. 27). The first part presents switching at z^+ surface under the electrode by correlated nucleation along the electrode edges, growth of isolated domains and their merging. The second part corresponds to the similar process at z^- by growth of the domains coming through the bulk. The third part is a result of the sideways motion of the walls at z^+ out of electrodes. The similar process at z^- gives the fourth part of the current. In this consideration

we neglect the input in the current of the charged domain walls motion in the bulk. For the domain wall motion out of electrodes we take into account its slowing due to dependence of local field at the wall on its shift (6).

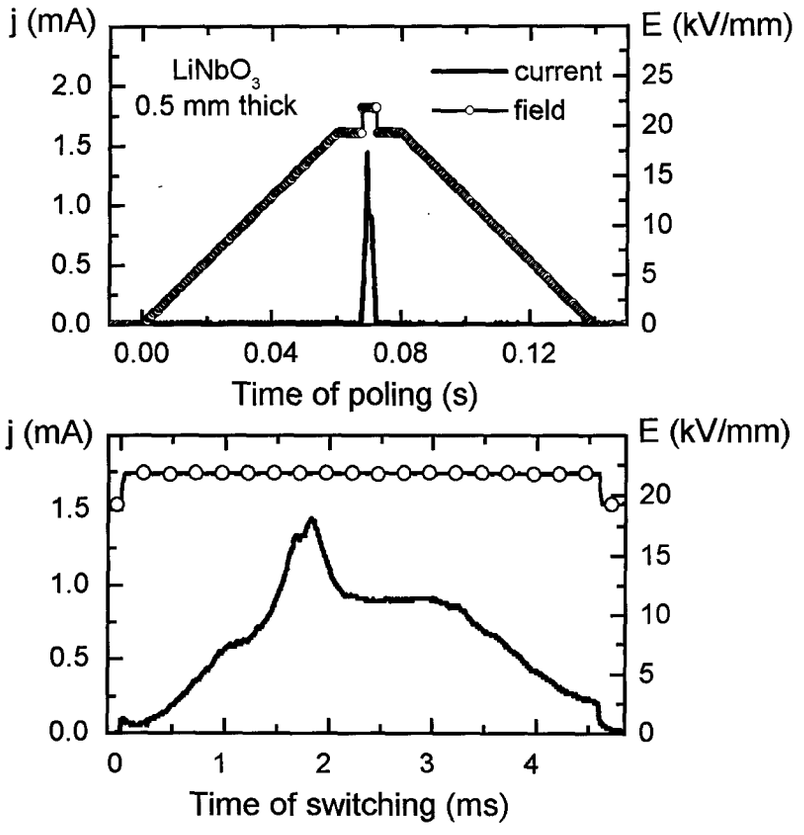

FIGURE 26 Field waveform and switching current for conventional poling.

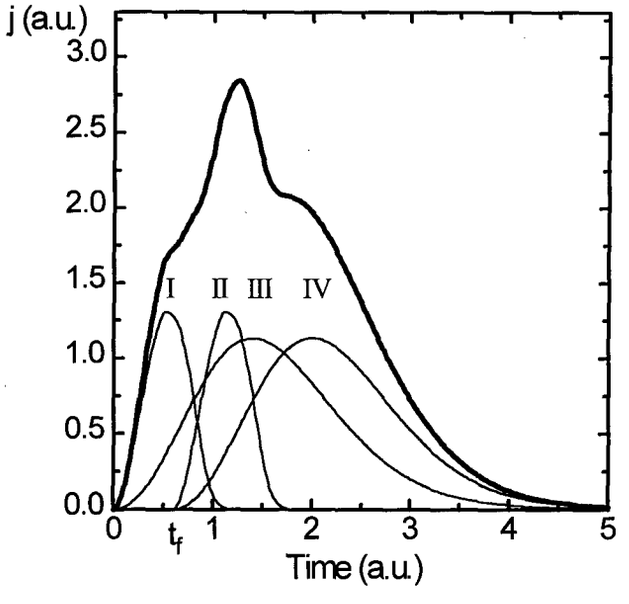

FIGURE 27 The scheme of the switching current with four inputs.

The fitting of experimental data is based on our modifications of Kolmogorov-Avrami formula for switching in finite media [23-25] with spatially nonuniform nucleation. The typical fitting of the experimental data using proposed approach is presented in Fig. 28. As a result we can clear extract two important moments of domain evolution. At the first one t_1 the isolated domains start to merge under the edges of electrodes. At the second moment t_2 the domains reach $\mathbf{z}^-$. It is clear that

$$t_1 = 0.5\ \Delta y/v_{ss} \tag{11}$$

$$t_2 = d/v_f \tag{12}$$

where Δy - the average distance between the nuclei,

v_{ss} - velocity of sideways domain growth under the edges of electrodes,

v_f - velocity of forward growth (tip propagation).

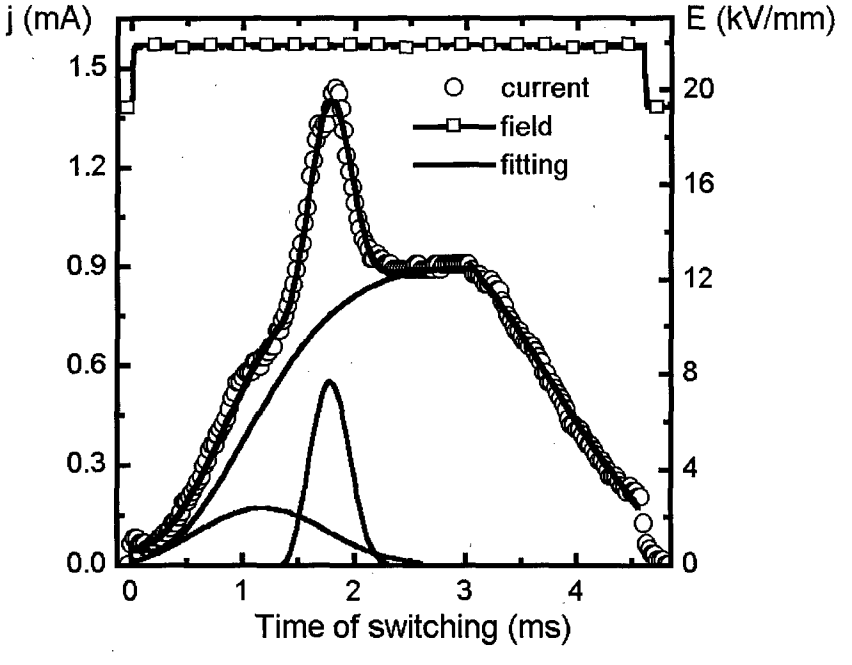

FIGURE 28 Switching current during poling. Experimental points were fitted by theoretical Equations based on modified Kolmogorov-Avrami theory [23-25].

The knowledge of these time intervals allows to determine the values of the most important velocities characterizing sideways domain wall motion and tip propagation. The results of the analysis of experimental data for about 10 samples with wide variety of electrode width and period are summarized in Table 4.

TABLE 4.

1	Forward growth velocity	304 ± 29 mm/s
2	Sideways velocity at electrode edges	0.51 ± 0.04 mm/s
3	Domain wall mobility	0.012 ±0.002 cm^2/Vs
4	Threshold field for poling	23.4 kV/mm
5	Threshold field for repoling	17.8 kV/mm

APPLICATION OF BACKSWITCHED POLING FOR 4 AND 2.6 μm PATTERNING

We apply the backswitching method for 4 μm periodical poling of the $LiNbO_3$ 0.5-mm-thick substrates. It is seen that the domain patterns on z^+ and z^- are practically ideal (Fig. 29 and 30). The cross-section shows that this structure is preserved through the bulk (Fig. 31). Such domain structure was prepared in whole 3 inch diameter substrate. It must be pointed out that to our knowledge to date attempts to produce the periodic domain structures with 4 μm period in 0.5-mm-thick $LiNbO_3$ by conventional poling method have not met with success.

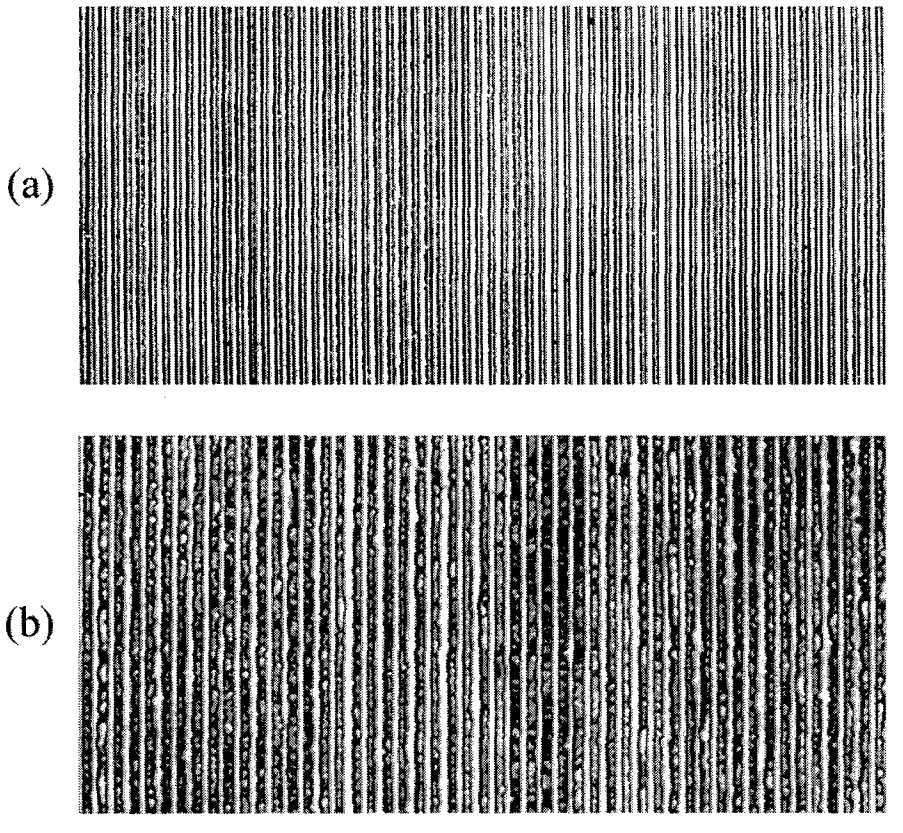

FIGURE 29 The domain patterns for 4 μm period for z^+ view with different magnification.

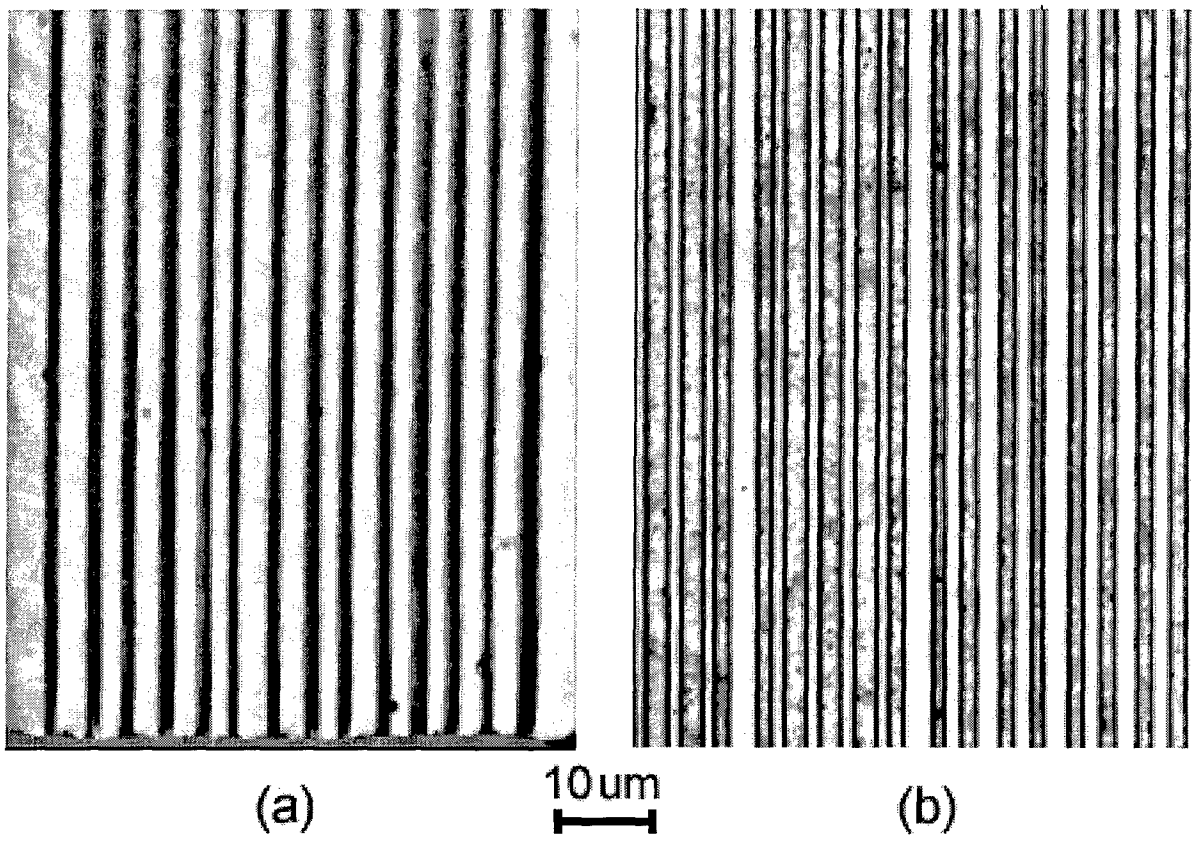

FIGURE 30 The domain patterns for 4 μm period for (a) **y** cross-section, (b) $\mathbf{z}^-$ view.

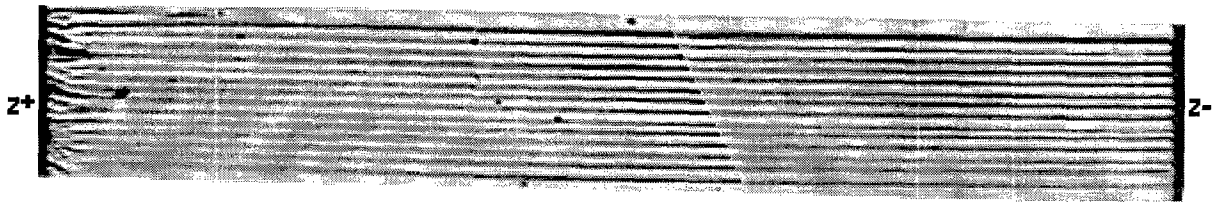

FIGURE 31 The domain patterns for 4 μm period for **y** cross-section.

The optimization of the poling conditions allows to produce 2.6 μm period domain structure in 0.5 mm thick wafer. In wide areas the ideal periodicity is observed at the both polar sides of the substrate (Fig. 32).

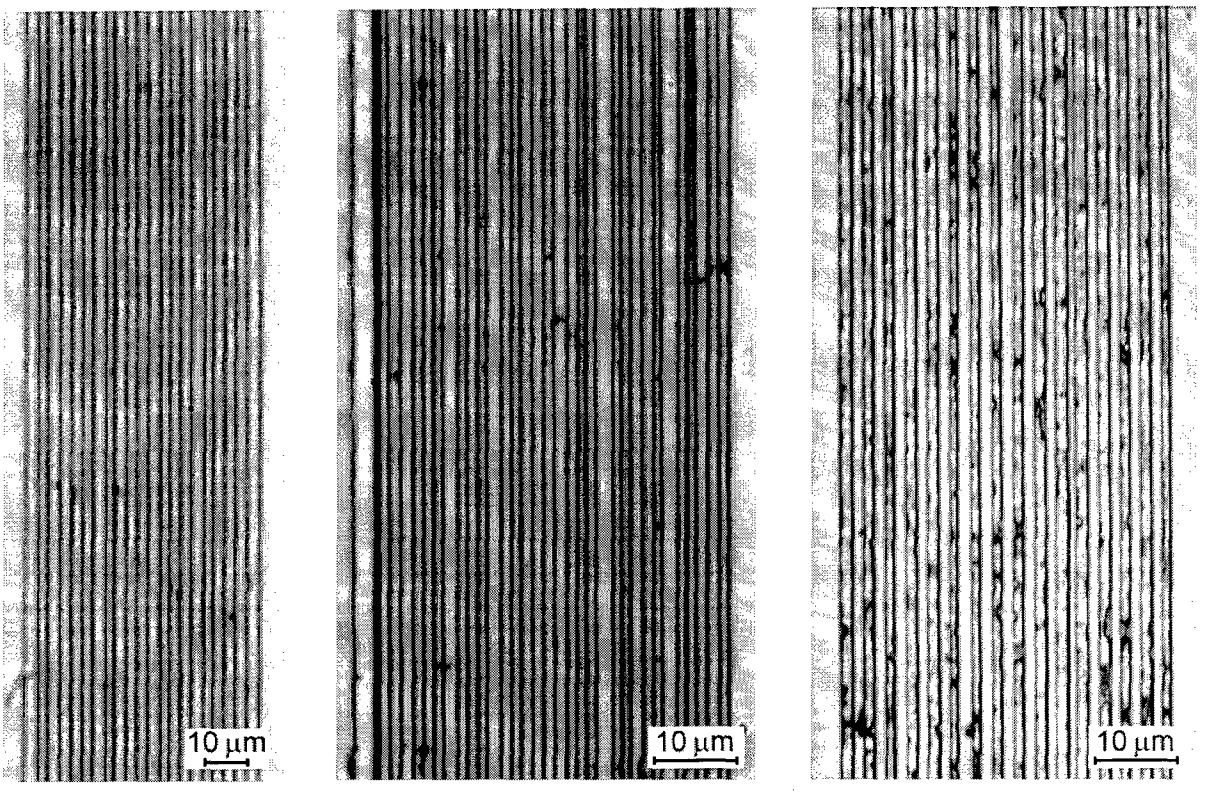

FIGURE 32 The domain patterns for 2.6 μm period for $\mathbf{z}^-$ view.

RECOMMENDATION

As a result of our investigations we have obtained the new important information about the domain kinetics in $LiNbO_3$ during poling. The detail information about domain kinetics during backswitching was obtained for the first time. It is shown that backswitched poling enables higher fidelity and shorter period bulk domain patterning in $LiNbO_3$ than can be achieved with conventional poling. The optimization of poling process allows to produce for the first time the bulk domain patterns with 4 and 2.6 μm period in 0.5-mm-thick substrates. The proposed technology based on the controlled backswitching process demonstrate the new possibilities in the domain engineering. The future progress in periodical patterning require the development of such activity for patterning of thicker substrates and to apply the proposed technique for $LiTaO_3$, and stoichiometric and doped $LiNbO_3$.

REFERENCES

1. R.L. Byer, "Quasi-Phasematched Nonlinear Interactions and Devices", Journal of Nonlinear Optical Physics & Materials, vol. 6, pp. 549-591, 1997.
2. M. Yamada, N. Nada, M. Saitoh, and K. Watanabe, "First-Order Quasi-Phase Matched $LiNbO_3$ Waveguide Periodically Poled by Applying an External Field for Efficient Blue Second-Harmonic Generation", Applied Physics Letters, vol. 62, pp. 435-436, February 1993.
3. J.U. Kang, W.K. Burns, Y.J. Ding, and J.S. Melinger, "First Observation of Backward Second-Harmonic Generation in Periodically Poled Bulk $LiNbO_3$", presented at the Conference on Lasers and Electro-Optics, Baltimore, Maryland, May 18-23, 1997.
4. K. Mizuushi and K. Yamamoto, "Generation of 340-nm Light by Frequency Doubling of a Laser Diode in Bulk Periodically Poled $LiTaO_3$", Optics Letters, vol. 21, pp. 107-109, January 1996.
5. J.-P. Meyn and M.M. Fejer, "Tunable Ultraviolet Radiation by Second-Harmonic Generation in Periodically Poled Lithium Tantalate", Optics Letters, vol. 22, pp. 1214-1216, August 1997.
6. W.P. Risk and S.D. Lau, "Periodic Electric Field Poling of $KTiOPO_4$ Using Chemical Patterning", Applied Physics Letters, vol. 69, pp. 3999-4001, December 1996.
7. V.Ya. Shur, in *Ferroelectric Thin Films: Synthesis and Basic Properties*, New York: Gordon&Breach, 1996, ch. 6, pp. 153-192.
8. L.E. Myers, R.C. Eckardt, M.M. Fejer, R.L. Byer, and W.R. Bosenberg, "Multigrating Quasi-Phase-Matched Optical Parametric Oscillator in Periodically Poled $LiNbO_3$", Optic Letters, vol. 21, pp. 591-593, April 1996.
9. G.D. Miller, R. G. Batchko, M. M. Fejer, and R. L. Byer, "Visible Quasi-Phasematched Harmonic Generation by Electric-Field-Poled Lithium Niobate", *SPIE Proceedings on Solid State Lasers and Nonlinear Crystals*, vol. 2700, 1996, pp. 34-36.
10. L.E. Myers, *Quasi-Phasematched Optical Parametric Oscillators In Bulk Periodically Poled Lithium Niobate*, Ph. D. thesis, The Stanford University, 1995.
11. G.D. Miller, R.G. Batchko, W.M. Tulloch, D.R Weise, M.M. Feier, and R.L. Byer, "42%-Efficient Single-Pass CW Second Harmonic Generation in Periodically Poled Lithium Niobate", Optics Letters, vol. 22, pp. 1834-1836, December 1997.
12. V.Ya. Shur, E.L. Rumyantsev, R.G. Batchko, G.D. Miller, M.M. Fejer, and R.L. Byer, "Physical Basis of the Domain Engineering in the Bulk Ferroelectrics", Ferroelectrics (in press).
13. V.Ya. Shur and E.L. Rumyantsev, "Kinetics of Ferroelectric Domain Structure: Retardation Effects", Ferroelectrics, vol.191, pp.319-333, 1997.
14. P.V. Lambeck, G.H. Jonker, "Ferroelectric Domain Stabilization in $BaTiO_3$ by Bulk Ordering of Defects", Ferroelectrics, vol. 22, pp.729-731, 1978.
15. V.M. Fridkin, *Ferroelectrics Semiconductors*, New York and London: Consultants Bureau, 1980, 264 p.
16. G.D. Miller, *Periodically Poled Lithium Niobate: Modeling, Fabrication, and Nonlinear-Optical Performance*, Ph. D. thesis, The Stanford University, 1998.

17. N. Ohnishi and T. Iisuka, "Etching Study of Microdomains in $LiNbO_3$ Single Crystals", Journal of Applied Physics, vol. 46, pp. 1063-1067, 1975.

18. V.Ya. Shur and E.L. Rumyantsev, "Crystal Growth and Domain Structure Evolution", Ferroelectrics, vol. 142, pp. 1-7, 1993.

19. V.Ya. Shur, A.L. Gruverman, V.V. Letuchev, E.L. Rumyantsev and A.L. Subbotin, "Domain Structure of Lead Germanate", Ferroelectrics, vol. 98, pp. 29-49, 1989.

20. V.Ya. Shur, A.L. Gruverman, V.P. Kuminov and N.A. Tonkachyova, "Dynamics of Plane Domain Walls in Lead Germanate and Gadolinium Molybdate", Ferroelectrics, vol. 111, pp. 197-206, 1990.

21. V.Ya. Shur, A.L. Gruverman, N.Yu. Ponomarev and N.A. Tonkachyova, "Change of Domain Structure of Lead Germanate in Strong Electric Field", Ferroelectrics, vol. 126, pp. 371-376, 1992.

22. V.Ya. Shur, A.L. Gruverman, N.Yu. Ponomarev, E.L. Rumyantsev and N.A. Tonkachyova, "Fast Reversal Process in Real Ferroelectrics", Integrated Ferroelectrics, vol. 2, pp. 51-62, 1992.

23. V.Ya. Shur, E.L. Rumyantsev, S.D. Makarov and V.V. Volegov, "How to Extract Information about Domain Kinetics in Thin Ferroelectric Films from Switching Transient Current Data", Integrated Ferroelectrics, vol. 5, pp. 293-301, 1994.

24. V.Ya. Shur, E.L. Rumyantsev, S.D. Makarov, A.L. Subbotin and V.V. Volegov, "Transient Current During Switching in Increasing Electric Field as a Basis for a New Testing Method", Integrated Ferroelectrics, vol. 10, pp. 223-230, 1995.

25. V.Ya. Shur, E.L. Rumyantsev and S.D. Makarov, "Investigation of Phase Transformation Kinetics in Real Finite Systems: Application to Ferroelectric Switching", Journal of Applied Physics, vol. 84, pp. 445-451, July 1998.

PRESENTATIONS

1. Vladimir Shur, Evgenii Rumyantsev, Robert Batchko, Gregory Miller, Martin Fejer and Robert Byer, Physical Basis of the Domain Engineering in the Bulk Ferroelectrics, Ferroelectrics (in press).
2. V.Ya. Shur, R.G. Batchko, E.L. Rumyantsev, G.D. Miller, M.M. Fejer, and R.L. Byer, Domain Engineering: Periodic Domain Patterning in Lithium Niobate, Proceedings of the XI IEEE International Symposium on the Applications of Ferroelectrics, 1998 (in press).
3. V.Ya. Shur, E.L. Rumyantsev, R.G. Batchko, G.D. Miller, M.M. Fejer, and R.L. Byer, Domain Kinetics during Periodic Domain Patterning in Lithium Niobate, Phys. Solid State (in press).
4. V.Ya. Shur, The Kinetic Nature of Ferroelectric Domain Patterns: Experiment, Simulation and Application, Bulletin of the American Physical Society, March 1998, V. 43, N 1, p. 375-376 (invited lecture).

5. V.Ya. Shur, On the Domain Engineering in Ferroelectrics, Abstracts of the 6th Japan/CIS/ Baltic Symposium on Ferroelectricity, Tokyo, Japan, March 22-26, 1998, p. 142 (invited lecture).
6. V.Ya. Shur, and E.L. Rumyantsev, Physical Basis of the Domain Engineering in the Bulk Ferroelectrics, Abstracts of International Symposium on Ferroic Domains and Mesoscopic Structures, State College, PA, April 6-10, 1998, p. 13 (invited lecture).
7. V.Ya. Shur, E.L. Rumyantsev, R.G. Batchko, G.D.Miller, M.M. Fejer, and R.L. Byer, Domain Engineering: Periodic Domain Patterning in Lithium Niobate, Abstract Book of the Joint International Conferences ISAF XI'98, ECAPD IV'98, Electroceramics VI'98, Montreux, Switzerland, August 24-27, 1998, p. 55 (invited lecture).
8. V.Ya. Shur, E.L. Rumyantsev, R.G. Batchko, G.D. Miller, M.M. Fejer, and R.L. Byer, Physical Basis of Periodic Domain Patterning in Lithium Niobate, 8th International Meeting on the Ferroelectrics - Semiconductors, Rostov-on-Don, Russia, 1998 (invited lecture).